



Hydrogen treatment of TiO₂ nanoparticles by DC plasma

M. Mashhadbani¹, M.R. Mohammadizadeh^{*1}, Y. Abdi²

¹ Supermaterials Research Laboratory (SRL), Department of Physics, University of Tehran, North Karegar Ave., P.O. Box 14395-547, Tehran, IRAN

² Nano-physics Research Laboratory, Department of Physics, University of Tehran, North Karegar Ave., P.O. Box 14395-547, Tehran, IRAN

ARTICLE INFO

Article history:

Received 17 July 2017
Revised 5 October 2017
Accepted 10 October 2017
Available online 20 October 2017

Keywords:

Nanostructures
H-plasma treatment
Photoluminescence
Catalytic properties

ABSTRACT

In this work structural defects were created in P25-TiO₂ nanoparticles by using hydrogen DC plasma treatment in different temperatures and exposure times. X-Ray diffraction measurements show that the structure of TiO₂ remains unchanged after hydrogenation. Diffuse reflectance spectroscopy measurements demonstrated that the band gap of TiO₂ was not changed considerably by the hydrogenation. However, by applying the hydrogen plasma for 40 min at a temperature of 350 °C, photocatalytic activity of TiO₂ nanoparticles enhances. No more change was observed in the photocatalytic activity of the samples with plasma exposure time more than 40 min. Photoluminescence analysis shows the sample prepared at 350 °C has a large amount of defects created by the plasma treatment. It seems both, structural defects and hydrogen doping in the samples are important for more efficient photocatalytic behavior of TiO₂ nanoparticles.

PACS: 82.45.Jn, 61.46.-w, 61.72.-y, 78.55.-m.

چکیده

در این مقاله از پودرهای TiO₂-P25 برای ایجاد نقص در شبکه دی اکسید تیتانیوم با روش پلاسمای هیدروژن DC بهبود یافته استفاده کردیم. خاصیت فوتوکاتالیستی با استفاده از متیلن بلو اندازه گیری شد. نتایج آزمایش فوتوکاتالیستی نشان دادند که بهترین زمان هیدروژن دهی ۴۰ دقیقه است. در نتایج تجربی، بهترین دما برای خاصیت فوتوکاتالیستی دمای 350°C به دست آمد. آنالیز PL بیشترین تعداد قله ها برای نقص های شبکه را در این دما به دست داد که نشان می دهد در این دما بیشترین درصد نقص های شبکه ای به وجود آمده است. نتایج XRD تغییر قابل ملاحظه ای در درصد فازهای آناتیس و روتایل نشان نمی دهد. نتایج DRS نیز تغییری در گاف انرژی نشان نداد.

اطلاعات مقاله

تاریخچه مقاله:

دریافت: ۲۶ تیر ۱۳۹۶

تصحیح: ۱۳ مهر ۱۳۹۶

پذیرش: ۱۸ مهر ۱۳۹۶

کلید واژگان:

نانوساختارها

پلاسمای هیدروژن

فوتولومینسانس

خواص کاتالیستی

*Corresponding author.

Email address: Zadeh@ut.ac.ir

DOI: 10.22051/JITF.2017.16459.1007

1 Introduction

TiO₂ has attracted a great deal of attention as Fujishima and Honda have published their research on it as a semiconductor photoelectrode in 1972 [1]. Chemical stability, nontoxic, low cost, and high photoactivity properties of TiO₂ are the most important factors which make it popular. In addition, it has a high dielectric constant and refractive index, and it is transparent in the visible light region. TiO₂ has important applications in many fields such as: solar cells [2-4], UV sensors [5], anode for lithium ion batteries [6], photocatalytic, and superhydrophilic properties in self-cleaning glasses [7,8]. Among crystal phases of TiO₂, anatase structure is the most active photocatalyst phase than the two other natural phases; rutile and brookite. Due to the large band gap of anatase TiO₂ 3.2 eV, it absorbs only the UV part of solar radiation. In recent years many researchers have tried to change its band gap energy like, doping with elements such as La [9], Pd [10], N [11-13], hydrogen [14-18], and also creating defects in TiO₂ structure [19,20]. Surface defects decrease recombination rate and prolong electron-hole (e-h) lifetime. Many investigations have been performed to recognize these defects. According to the reported results, it seems the dominant defects on TiO₂ surface are Ti³⁺ and oxygen vacancies (OV) [21,22]. Some of the methods to create defects in the TiO₂ are annealing at temperatures above 400 °C [23-26], reducing with hydrogen [22,27,28] or CO [29], ion bombardment [26,30], and UV exposure [31].

As it was already mentioned, hydrogen is one of the elements which can improve photocatalytic activity of TiO₂. Hydrogen in TiO₂ structure can decrease the band gap energy, or it can create defects in the structure [15]. There are some approaches to introduce hydrogen in TiO₂ structure; References [20,32] have used rf-plasma and Ref. [19] has used thermal hydrogen treatment to create defects in TiO₂ structure and reported defects caused to enhance photocatalytic activity. In this work we have reduced P25-TiO₂ using hydrogen DC plasma treatment. We have used low temperatures and plasma pressure for hydrogenation treatment, and investigated its effects on photocatalytic activity of TiO₂ nanoparticles.

2 Experimental details

P25-TiO₂ was used as a reference for photocatalytic studies. It is a well-known material for its high photoactivity; due to proper mixture of anatase and rutile phases the separation between electrons and holes has been optimized to enhance photocatalytic activity. The P25 consists of approximately 80% anatase and 20% rutile nanoparticles with about 25 nm diameter size. We have reduced TiO₂ powder using DC plasma hydrogenation treatment. TiO₂ powder was put in a boat and placed inside the cylindrical quartz reactor under 2×10⁻² Torr vacuum pressure. Then H₂ gas was introduced into the reactor with flow rate at 0.2 lit/min. Plasma power density was about 2 W/cm². Plasma treatment was carried out at different temperatures and exposure times. It was observed that the color of P25 powder changed from white to beige after hydrogenation. This color change is due to OVs at surface of TiO₂ [33,34]. With increasing plasma exposure time up to 40 min, the color of the samples gets more intense. However, more than this exposure time, at t=60 min, no change in the color of samples was observed. Figure 1 shows the powder after 40 min hydrogenation at temperature T =350°C.



Fig. 1: P25-TiO₂ powder after hydrogenation at $\Delta t=40$ min plasma exposure time and temperature $T=350$ °C.

XRD (PHILIPS PW3040/60) at 40 kV and 30 mA current was employed to TiO₂ and 2θ was in the range between 10-60°. Diffuse reflectance spectroscopy (DRS) was used to evaluate the band gap energy (Light source: AvaLight DH-S, vaSpec2048Tec). Photocatalytic activity was evaluated by detecting the degradation rate

of Methylene blue (MB); 30 mg of TiO₂ was dispersed into 30 mL of 0.001 M Methylene blue solution. A mercury lamp was used as a UV source with an intensity of 2.5 mW/cm² on the sample. The suspension was stirred constantly under the light irradiation. The mixture was centrifuged after 10 min and the transmittance was measured with UV-Vis spectrophotometer (RYE UNICAN). Photoluminescent (PL) spectroscopy (Avantes) was performed to detect surface defects, too. The excitation source for PL spectroscopy was a 380 nm diode source.

3 Results and discussion

We have measured the XRD spectrum for 4 samples, including pure P25 and the hydrogenated P25 at Δt=40 min at three different temperatures: T= 300 °C, 350 °C, and 400 °C. Figure 2 illustrates the XRD patterns of these samples. As this figure indicates, there is no change in the structure and phases of TiO₂ after hydrogenation, and no additional phase is observed. This result shows the lattice structure is preserved during the hydrogenation process.

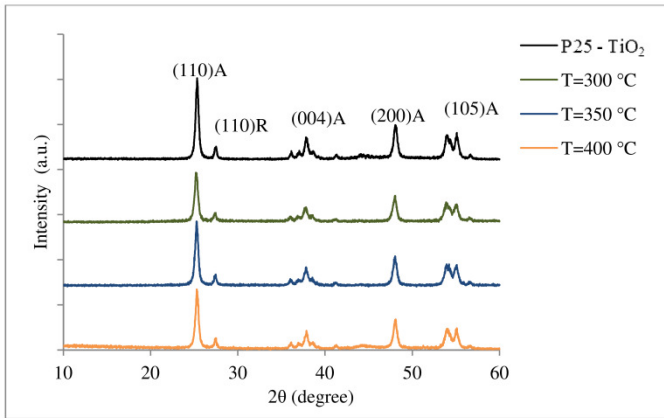


Fig. 2: XRD patterns of P25-TiO₂ and hydrogenated one at different temperatures at Δt=40 min plasma exposure time.

Using intensities of peaks and the following formulas, the ratio of anatase and rutile phases was calculated [35];

$$A = \frac{0.8I_A}{I_R + 0.8I_A} \times 100, \quad (1)$$

$$R = \frac{1}{1 + 0.8 \left(\frac{I_A}{I_R}\right)} \times 100, \quad (2)$$

where A and R are the percent amount of anatase and rutile phases, and I_A and I_R are the heights of the major peaks of anatase and rutile phases, respectively. Table 1 presents the measured values. The results indicate that after hydrogenation, the amount of anatase phase is increased but this value is negligible. This is in agreement with other previous reports [33,36]. Although, it can be seen that the most concentration of anatase is created in T=350 °C, which it has more photocatalytic activity.

Table 1: The measured values of anatase and rutile phases concentrations for P25-TiO₂ and hydrogenated P25-TiO₂ under 40 min plasma treatment at different temperatures.

Sample	Anatase (%)	Rutile (%)
P25-TiO ₂	81	19
T=300 °C	84	16
T=350 °C	86	14
T=400 °C	83	17

DRS measurement was used to measure the optical properties of TiO₂ samples. We can evaluate the band gap energy from DRS results. To evaluate band gap energy E_g, we have used Kubelka-Munk function [37];

$$F(R) = \frac{K}{S} = \frac{1 - R^2}{2R}, \quad (3)$$

where K is the absorption coefficient, S is the scattering coefficient, R is the reflectance, and F(R) is the Kubelka-Munk function. To measure E_g, the plot of (F(R)hv)^{1/2} vs. hv (incident photon energy) was drawn. The intersection point of the tangent line with hv axis is E_g. Figures 3 and 4 show (F(R)hv)^{1/2} vs. hv for different hydrogenation exposure times and temperatures.

As it can be seen from these figures, the band gap energy was decreased slightly after hydrogenation of the samples. Tables 2 and 3 illustrate the measured values of E_g. As Tables 2 and 3 represent, there is a slight decrease in E_g values with increasing hydrogenation exposure time and temperature.

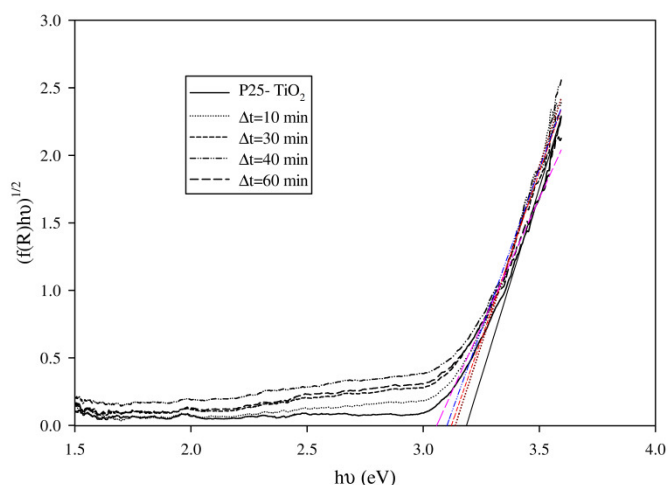


Fig. 3: $(F(R)hv)^{1/2}$ vs. photon energy for P25-TiO₂ and the samples with different hydrogenation exposure times at constant temperature T=350 °C.

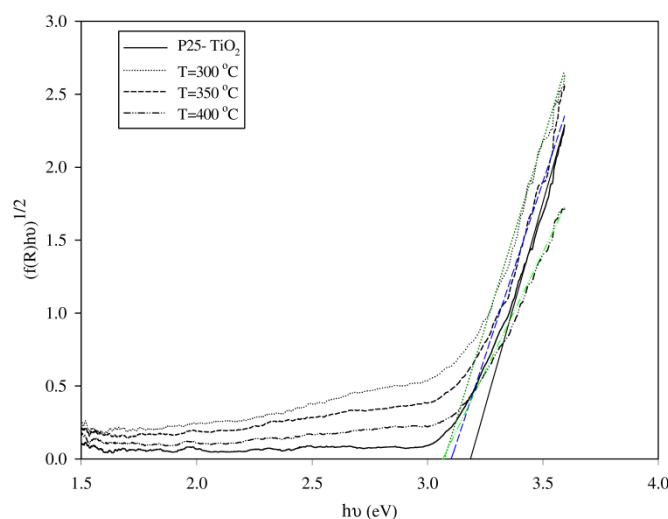


Fig. 4: $(F(R)hv)^{1/2}$ vs. photon energy for P25-TiO₂ and the samples with different hydrogenation temperatures and constant plasma exposure time $\Delta t=40$ min.

However, these changes of E_g due to the plasma treatment are not significant, which is in agreement with another report [19].

Photocatalytic activity of hydrogen treated TiO₂ nanoparticles was evaluated by degradation of MB under UV irradiation. Figure 5 shows degradation of MB for samples at different hydrogenation exposure times and constant temperature T=350°C. Degradation rate of MB has increased with increasing of hydrogenation exposure time up to t=40 min.

Table 2: Band gap energy for P25-TiO₂ and samples under T=350 °C plasma temperature with different hydrogenation exposure times.

Sample	E_g (eV)
P25-TiO ₂	3.19
$\Delta t=10$ min	3.14
$\Delta t=30$ min	3.12
$\Delta t=40$ min	3.10
$\Delta t=60$ min	3.06

Table 3: Band gap energy for P25-TiO₂ and samples under $\Delta t=40$ min of plasma treatment with different hydrogenation temperature.

Sample	E_g (eV)
P25-TiO ₂	3.19
T=300 °C	3.07
T=350 °C	3.10
T=400 °C	3.06

However, when the hydrogenation exposure time has increased to t=60 min, no change was observed in the degradation rate. This result demonstrates that the best hydrogenation exposure time for photocatalytic activity of the sample is $\Delta t=40$ min in our plasma conditions.

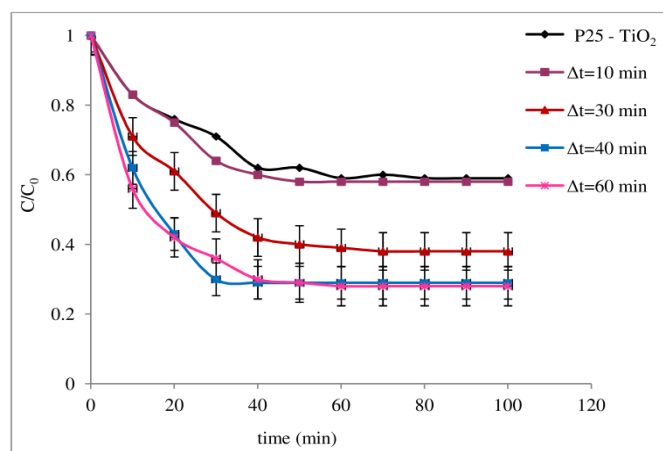


Fig. 5: Photocatalytic degradation of MB for P25-TiO₂ and samples with different hydrogenation exposure times at constant temperature T=350 °C.

It may be concluded with increasing hydrogenation exposure time more than $\Delta t=40$ min, the amount of defects remains constant and as a result, the photocatalytic activity is not improved any more.

Many factors affect the photocatalytic activity that one of them is defect. Separation of the electron-hole pair plays a predominant role in photocatalytic reaction. Defects can decrease the recombination rate between electrons and holes and increase the electron-hole lifetime, where as a result the photocatalytic activity is increased [19]. There are some methods to trace the defects such as PL.

Measurement of PL emission was performed to study defects of the samples with different hydrogenation exposure times at constant temperature $T=350$ °C (Fig. 6). There are two types of PL peaks. The band-band peaks are at wavelengths about $\lambda=380$ nm [36,38], which we have not observed. This peak was ascribed to the emission of band gap transition. As it can be seen from Fig. 6, P25-TiO₂ shows one peak at $\lambda=530$ nm. Some other peaks appeared after hydrogen treatment. At time $\Delta t=10$ min sample, there are two peaks at $\lambda=540$ nm and $\lambda=560$ nm (2.30 and 2.21 eV, respectively).

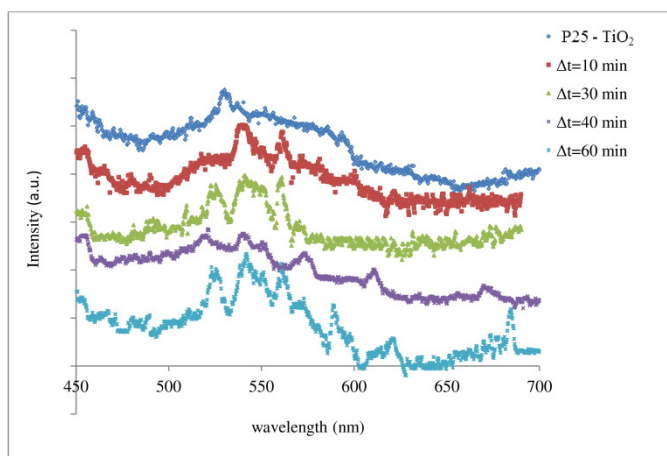


Figure 6: The PL spectra of P25-TiO₂ and hydrogenated samples at different plasma exposure times and constant temperature $T=350$ °C.

For hydrogenation exposure time $\Delta t=30$ min, three peaks at $\lambda=520$, 540, and 560 nm (2.39, 2.30, and 2.21 eV, respectively) appeared. TiO₂ with hydrogenation exposure time $\Delta t=40$ min shows six peaks at $\lambda=520$, 540, 550, 570, 610, and 670 nm (2.39, 2.30,

2.26, 2.18, 2.04, and 1.85 eV, respectively). At $\Delta t=60$ min sample, there are six peaks at $\lambda=520$, 540, 560, 590, 620, and 685 nm (2.39, 2.30, 2.21, 2.10, 2.00, and 1.81 eV, respectively). Both of the later samples show six peaks at wavelengths between $\lambda=450-700$ nm. Positions of the peaks at $\Delta t=60$ min sample showed a red shift with respect to the peaks observed at $\Delta t=40$ min, which could be due to the larger particle sizes [39]. The number of peaks did not change by increasing the hydrogenation exposure time from 40 min to 60 min. We can conclude that the defect concentration was not changed, so photocatalytic activity remains constant with increasing the hydrogenation time from 40 to 60 min. According to the photocatalytic results we can conclude that the hydrogenation exposure time 40 min is the optimum time for photocatalytic activity and in time beyond it, photocatalytic activity remains unchanged.

To determine the optimum temperature for photocatalytic activity three samples were made in different hydrogenation temperatures $T=300$, 350, and 400 °C at constant plasma exposure time $\Delta t=40$ min. We have presented photocatalytic activity of the samples at different hydrogenation temperatures in Fig. 7. Degradation rate of MB is increased with increasing the hydrogenation temperature from $T=300$ °C to $T=350$ °C. However, when the plasma temperature is increased to $T=400$ °C, the degradation rate decreases. Therefore, hydrogenation temperature $T=350$ °C is the optimum temperature.

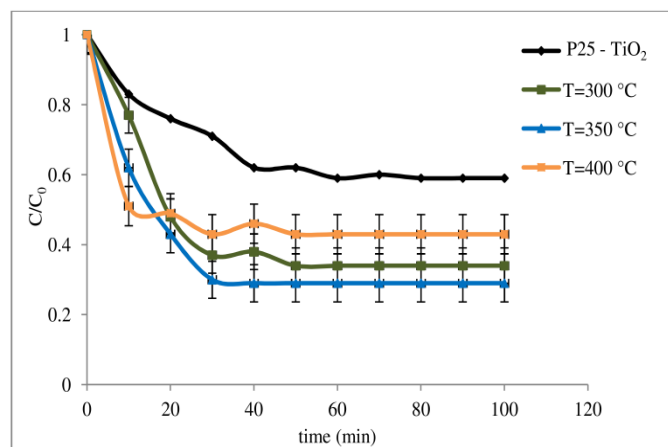


Fig. 7: Photocatalytic degradation of MB for P25-TiO₂ and hydrogenated samples at different temperatures and constant plasma exposure time $\Delta t=40$ min.

The structural incompleteness due to the plasma treatment could be relaxed more in higher temperatures [33].

Figure 8 shows PL spectra of the P25-TiO₂ and the hydrogenated samples at different temperatures. P25-TiO₂ exhibits one peak at wavelength $\lambda=530$ nm (2.34 eV). P25-TiO₂ at $\Delta t=40$ min and $T=300$ °C shows three peaks at $\lambda=540, 560,$ and 610 nm (2.30, 2.21, and 2.04 eV, respectively). Sample at $T=350$ °C shows six peaks at $\lambda=520, 540, 570, 590, 610,$ and 675 nm (2.39, 2.30, 2.18, 2.10, 2.04, and 1.84 eV, respectively). As the temperature increases to $T=400$ °C the number of peaks is decreased showing four peaks at $\lambda=515, 540, 610,$ and 660 nm (2.41, 2.30, 2.04, and 1.88 eV, respectively). The position of PL spectrum peak depends on the lattice structure of TiO₂ and concentration of defects [38,40-42].

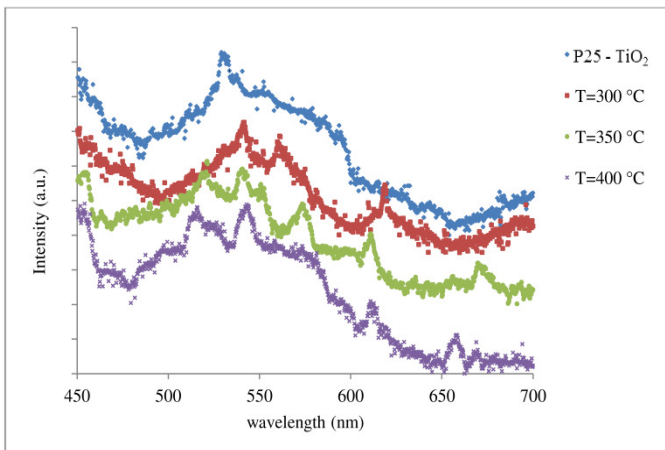


Fig. 8: Photoluminescence spectra of P25-TiO₂ and hydrogenated ones at plasma exposure time $\Delta t=40$ min and different temperatures.

According to PL results we can conclude that the hydrogenated P25-TiO₂ sample at $T=350$ °C may have the maximum amount of defects. As the temperature was increased to $T=400$ °C, defects were decreased, and as a result, photocatalytic activity was decreased. Decreasing photocatalytic activity with increasing of hydrogenation temperature has already been reported [19, 33]. The defects of TiO₂ decrease the recombination rate of e-h pairs, prolong e-h pair lifetime, and therefore enhance the photocatalytic activity. As already reported [33],

with increasing temperature, the created defects are transferred from the surface of TiO₂ to the bulk, i.e. surface defects intensity is decreased. The peaks in wavelengths $\lambda=440-570$ nm (with the energy range 2.2-2.8 eV) are associated with the excitations due to oxygen vacancies [38,40]. The peaks with wavelengths between $\lambda=670-710$ nm (with the energy range 1.75-1.85 eV) are attributed to the emission from Ti³⁺ defects [40]. All the samples show peaks in wavelengths between 440-570 nm which shows that the OV defects are created in all the samples. However, some other peaks appeared with increasing of the plasma exposure time and temperature up to $\Delta t=40$ min and $T=350$ °C, respectively. According to PL results, we can conclude when TiO₂ is hydrogenated, at first OV defects are created. Then with increasing the hydrogenation exposure time to $\Delta t=40$ min, Ti³⁺ peaks are also created and these defects remain in the structure when hydrogenation time is even increased. In hydrogenation exposure time $\Delta t=40$ min, the Ti³⁺ peak is observed as temperature is increased to $T=350$ °C. When the temperature was increased to $T=400$ °C, the peak corresponding to Ti³⁺ defects still exists but the number of peaks corresponding to OV defects is decreased and photocatalytic activity is decreased. It is known that both OV and Ti³⁺ defects play a role in photocatalytic activity [43], but we cannot determine exactly which of them is created in reduction with hydrogen plasma.

4 Conclusions

P25-TiO₂ powder was reduced with DC plasma hydrogen treatment in different plasma exposure times and temperatures. Our results represent a significant improvement in photocatalytic activity of the samples. XRD results show that the structure of TiO₂ was not changed after hydrogenation. No significant change was observed in the band gap energy using DRS spectra. An optimum time and temperature of hydrogenation treatment for photocatalytic activity was found at time $\Delta t=40$ min and temperature $T=350$ °C. Based on PL results, more concentration of defects is created in this temperature. Lattice defects influence the photocatalytic activity by increasing e-h recombination lifetime. This could be due to the local states originated from Ti³⁺ and OV defects.

Acknowledgments

Partial financial support by the research council of the University of Tehran and “center of excellence on the structure and physical properties of matter” of the University of Tehran are acknowledged. Mohammadzadeh would also like to thank the Abdus Salam International Center for Theoretical Physics (ICTP) for good hospitality during preparation of this article.

References

- [1] A. Fujishima, K. Honda, *Nature* **238** (1972) 37.
- [2] P. J. Cameron, L. M. Peter, *J. Phys. Chem. B* **107** (2003) 14394.
- [3] M. Okuya, K. Nakade, S. Kaneko, *Sol. Energy. Mate. Sol. Cell.* **70** (2002) 425.
- [4] M. Okuya, K. Nakade, D. Osa, T. Nakano, G. R. A. Kumara, S. Kaneko, *J. Photochem. Photobio. A: Chemistry* **164** (2004) 167.
- [5] M. Okuya, K. Shiozaki, N. Horikawa, T. Kosugi, G.R.A. Kumara, J. Madarász, S. Kaneko, G. Pokol, *Solid State Ionic* **172** (2004) 527.
- [6] C. Natarajan, N. Fukunaga, G. Nogami, *Thin Solid Films* **322** (1998) 6.
- [7] M. Kazemi, M. R. Mohammadzadeh, *Chem. Engineer. Res. Des.* **90** (2012) 1473; M. Kazemi, M. R. Mohammadzadeh, *Thin Solid Films* **519** (2011) 6432.
- [8] M. Kazemi, M. R. Mohammadzadeh, *Appl. Surf. Sci.* **257** (2011) 3780; A. A. Ashkarran, M. R. Mohammadzadeh, *Mater. Res. Bull.* **43** (2008) 522.
- [9] C. Wen, D. Hua, T. Jun-ying, A. Ji-Mei, *Trans. Nonferrous Met. Soc. China* **16** (2006) 728.
- [10] Y. Zhu, Li. Zhang, W. Yao, L. Cao, *Appl. Surf. Sci.* **158** (2000) 32.
- [11] D. Li, H. Haneda, S. Hishita, N. Ohashi, *Chem. Mater.* **17** (2005) 2588.
- [12] C. Huang, L. Chen, K. Cheng, G. Pan, *J. Mol. Catal. A: Chemical* **261** (2007) 218.
- [13] M. Chekini, M.R. Mohammadzadeh, S.M. Vaez Allaei, *Appl. Surf. Sci.* **257** (2011) 7179 ; S. Kimyagar, M. R. Mohammadzadeh, *Euro. Phys. J. Appl. Phys.* **61** (2013) 10303.
- [14] W. P. Chen, Y. Wang, H. L. Chan, *Appl. Phys. Lett.* **92** (2008) 112907; S. Hidari, M. R. Mohammadzadeh, M. Mahjour-Shafiei, M. M. Larijani, M. Malek, *Appl. Phys. A* **121** (2015) 149; M. R. Mohammadzadeh, M. Bagheri, S. Aghabagheri, Y. Abdi, *Appl. Surf. Sci.* **350** (2015) 43.
- [15] X. Chen, L. Liu, P. Y. Yu, S. S. Mao, *Science* **331** (2011) 746; M. Sotudeh, M. Abbasnejad, M.R. Mohammadzadeh, *Euro. Phys. J. Appl. Phys.* **67** (2014) 30401; M. Sotudeh, S. J. Hashemifar, M. Abbasnejad, M.R. Mohammadzadeh, *AIP Advances* **4** (2014) 027129.
- [16] C. Sun, Y. Jia, X. Yang, H. Yang, H. G. Yang, X. Yao, G. Lu, A. Selloni, S. C. Smith, *J. Phys. Chem. C* **115** (2011) 25590.
- [17] F. Herkoltz, E. V. Lavrov, J. weber, *Phys. Rev. B:* **83** (2011) 235202.
- [18] C. Kilic, A. Zunger, *Appl. Phys. Lett.* **81** (2002) 73.
- [19] H. Liu, H. T. Ma, X. Z. Li, W. Z. Li, M. Wu, X. H. Bao, *Chemosphere* **50** (2003) 39.
- [20] T. Ihara, M. Miyoshi, *J. Mater. Sci.* **36** (2001) 4201.
- [21] K. Suriye, B. Ch. Satayaprasert, P. Praserttham, *Appl. Surf. Sci.* **255** (2008) 2759.
- [22] V. Henrich, R. L. Kurtz, *Phys. Rev. B* **23** (1981) 6280.
- [23] G. Lu, A. Linsebigler, J.T. Yates, *J. Chem. Phys.* **98** (1994) 11733.
- [24] W. Gopel, J.A. Anderson, D. Frankel, M. Jaehnig, K. Phillips, J.A. Schafer, G. Rocker, *Surf. Sci.* **139** (1984) 333.

- [25] J.M. Pan, B.L. Maschoff, U. Diebolt, T.E. Madey, *J. Vac. Sci. Technol. A* **10** (1992) 2470.
- [26] Q. Zhong, J. M. Vohs, D. A. Bonnell, *Surf. Sci.* **274** (1992) 35.
- [27] Z. Zhang, S. P. Jeng, V. E. Henrich, *Phys. Rev. B* **43** (1991) 12004.
- [28] Q. Zhong, J. M. Vohs, D. A. Bobbell, *J. Am. Ceram. Soc.* **76** (1993) 1137.
- [29] W. Gopel, G. Rocker, R. Feirabend, *Phys. Rev. B* **28** (1983) 3427.
- [30] V. E. Hemrich, G. Dresselhaus, H. Zeiger, *Phys. Rev. Lett.* **36** (1976) 1335.
- [31] A. N. Shultz, W. Jang, W. M. Hetherington, D. R. Baer, L. Q. Wang, M. H. Engelhard, *Surf. Sci.* **339** (1995) 114.
- [32] Y. K. Chae, S. Mori, M. Suzuki, *Thin Solid Films* **517** (2009) 4260.
- [33] T. Leshuk, R. Parviz, P. Evert, H. Krishakumar, R.A. Varin, F. Gu, *Appl. Mater. Interf.* **5** (2013) 1892.
- [34] U. Diebold, *Surf. Sci. Reports* **48** (2003) 53.
- [35] R. A. Spurr, H. Myers, *Analyt. Chem.* **29** (1957) 760.
- [36] X. Jiang, Y. Zhang, J. Jiang, Y. Rong, Y. Wang, Y. Wu, C. Pan, *J. Phys. Chem. C* **116** (2012) 22619.
- [37] R. Trejo-Tzab, J. J. Alvarado-Gil, P. Quintana, *Top Catal.* **54** (2011) 250.
- [38] G. Zhu, T. Lin, X. Lü, W. Zh, C. Yang, Z. Wang, H. Yin, Z. Liu, F. Q. Huang, J. Lin, *J. Mater. Chem. A* **1** (2013) 9650.
- [39] X. Chunxiang, X. Quinghua, Z. Yuan, C. Yiping, B. Lang, Z. Bing, G. Ning, *Nanotechnology* **13** (2002) 47.
- [40] Y. Zhang, J. Li, J. Wang, *Chem. Mater.* **18** (2006) 2917.
- [41] W. Dong, G. Pang, Z. Shi, Y. Xu, H. Jin, R. Shi, J. Ma, S. Feng, *Mater. Res. Bull.* **39** (2004) 433.
- [42] N. Serpone, D. Lawless, R. Khairutdinov, *J. Phys. Chem.* **99** (1995) 16646.
- [43] C. Di Valentin, G. Pacchioni, *J. Phys. Chem. C* **113** (2009) 20543.